Available online at www.sciencedirect.com
SCIENCE DIRECT
Catalysis Today 107–108 (2005) 545–550
CATALYSIS TODAY
www.elsevier.com/locate/cattod

Hydrodemetallation (HDM) kinetics of Ni-TPP over Mo/Al_2O_3-TiO_2 catalyst

A.J. García-López [a], R. Cuevas [a,*], J. Ramírez [a,b], J. Ancheyta [b], A.A. Vargas-Tah [a], R. Nares [b], A. Gutiérrez-Alejandre [a]

[a] *UNICAT, Facultad de Química, UNAM, L-225 Conjunto "E", Facultad de Química, 04510 Coyoacán, México D.F., México*
[b] *Instituto Mexicano del Petróleo, Eje Central Lázaro Cárdenas 152, México D.F. 07730, México*

Available online 19 August 2005

Abstract

The intrinsic hydrodemetallation (HDM) kinetics of nickel 5,10,15,20-tetraphenylporphyrin (Ni-TPP), was studied over a sulfided Mo catalyst supported on a mixed oxide alumina-titania (Mo/Al_2O_3-TiO_2), with a controlled pore distribution. This work analyses the effects of using an Al_2O_3–TiO_2 support, on the reaction steps of Ni-TPP hydrodemetallation. The HDM reaction was carried out in a batch reactor at 325 °C and 8.3 MPa of total hydrogen pressure, using nujol as solvent. Under these conditions, it was determined that Ni-TPP reacts through a sequential mechanism. In the first step, Ni-TPP is reversibly hydrogenated to nickel 5,10,15,20-tetraphenylchlorin (Ni-TPC); this compound was then hydrogenated to nickel 5,10,15,20-tetraphenylisobacteriochlorin (Ni-TPiB). Finally, the Ni-TPiB reacts via a series of fast reactions, ending in demetallation and ring fragmentation. This mechanism is similar to the previously reported HDM mechanisms for Ni-TPP. However, the controlling step for the HDM rate was the first hydrogenation of Ni-TPP instead of the reported hydrogenolysis step. This change in controlling step was ascribed to the support influence and was explained on the basis of the surface acidity of the catalysts.

Keywords: HDM; Nickel tetraphenylporphyrin; Kinetics; Mixed oxides; Al_2O_3–TiO_2

1. Introduction

The increasing consumption of fuels and the availability of heavy petroleum have compelled refiners not only to process a higher amount of oil but also increasing amounts of heavy crude, in order to fulfill the demand for gasoline and diesel. This fact, therefore, increases the level of hydrotreating (HDT) of the high molecular weight residuum. These residua contain high amounts of several polluting agents, such as sulfur, nitrogen and metals. Among these metals, the most abundant and problematic, without any doubt, are vanadium and nickel. Depending on the origin of the crude, the concentration of vanadium commonly varies between 8 and 1200 ppm (weight), whereas nickel varies between 4 and 150 ppm. Specifically, vanadium and nickel compounds cause severe problems in the hydrodesulfurization (HDS) and catalytic cracking reactors. In the HDS units, these metals are deposited on the catalyst as metal sulfides. The metal deposits poison the active sites, obstruct the pores entrance and finally determine the lifetime for the catalyst [1]. Clearly, a sufficient knowledge of the kinetics of Ni and V hydrodemetallation is very important for the improvement and development of better catalysts and reactors for HDM.

Various researchers have studied the kinetics for the removal of metals with diverse types of crude, and still a certain dispute exists over the right reaction order. For example, in typical HDS ($CoMo/Al_2O_3$) catalysts reacting in hydrogen presence, second [2] and first [3] orders have been reported. The main reason for this inconsistency appears to be the presence of diverse heteroatoms in the crude, whose nature and relative amount still lack identification and quantification.

HDM kinetic studies have been usually made using model molecules. The use of model molecules provides a useful way to understand the reactions that occur in HDM

* Corresponding author.
E-mail address: cuevas@servidor.unam.mx (R. Cuevas).

0920-5861/$ – see front matter © 2005 Elsevier B.V. All rights reserved.
doi:10.1016/j.cattod.2005.07.104

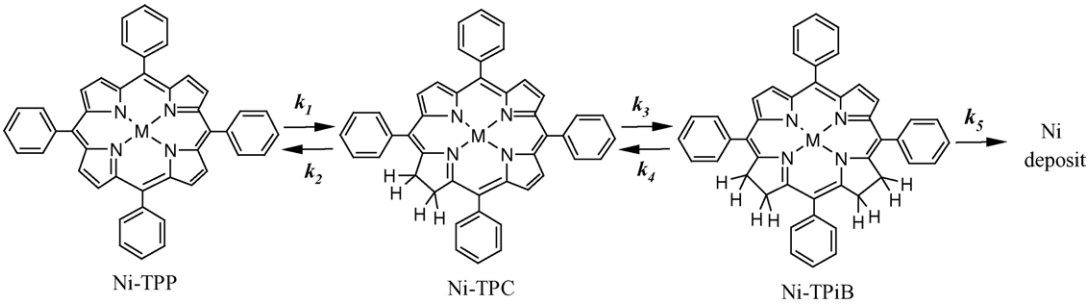

Fig. 1. Reaction pathway for Ni-TPP HDM.

processes because the chemical analyses of reactants, intermediates and final products are easily figured out.

Three types of nickel or vanadium porphyrins are used more frequently as model compounds in HDM studies because they are representative of the real molecules in the crude, they are: etioporphyrins (Etio type), tetraphenylporphirins (TPP) and tetra(3 metil-phenyl)porphyrins. It was Wei et al. [4–7] who made the first HDM kinetic studies with model compounds. Later Chen [8] and Bonné [9] conducted additional studies. Working with Etio type porphyrines Hung [4] observed fractional kinetic orders, respect to the total metal concentration. Values of these orders varied with the temperature and operating hydrogen pressure. Later, Agrawal [5] proposed consecutive reaction kinetics for the HDM of Etio type porphyrins. The proposed model includes a reversible hydrogenation and an irreversible hydrogenolysis steps. Later, Ware [6] and Smith [7] confirmed this consecutive mechanism. In contrast, studies performed with TPP type porphyrines [6,9] indicated that TPP reacts through a consecutive mechanism with two reversible hydrogenation and irreversible hydrogenolysis steps, as is shown in Fig. 1.

The previous investigations of HDM kinetics with model compounds were made with Mo or CoMo based catalysts, always supported in γ-alumina (γ-Al_2O_3). The influence of other types of supports on the kinetics of HDM has not yet been addressed. It has been reported that Ti-containing HDS catalysts perform better in hydrotreating processes due to a promoting effect and also because of the semiconductor character of TiO_2 [10]. In this line, the objective of this work is to investigate the intrinsic HDM kinetics of nickel 5,10,15,20-tetraphenylporphyirin (Ni-TPP) with a Mo catalyst supported on an alumina-titania mixed oxide (Mo/Al_2O_3-TiO_2), with bimodal pore size distribution.

2. Experimental

2.1. Support preparation

The Al_2O_3–TiO_2 support, with 1:1 molar ratio, Al_2O_3/(TiO_2+Al_2O), was prepared by the ''sol–gel method'' using aluminum isopropoxide (AIP) and titanium isopropoxide (TIP) as metal precursors and *n*-propanol as solvent. To obtain a bimodal porous system $(NH_4)_2CO_3$ was added in aqueous solution to the synthesis mixture. The resulting precipitate was filtered and washed with water, dried at 100 °C for 24 h and calcined at 500 °C by 24 h. The synthesized support showed bimodal pore size distribution with maximum adsorption volume at pore diameters of 100 and 300 Å and specific area of 287 m^2/g. In Fig. 2 the pore volume distribution for the synthesized support is displayed. Additionally, an Al_2O_3 support was prepared as reference support using the same method formerly described without ammonium carbonate and TIP additions.

2.2. FT-IR of adsorbed pivalonitrile (PN)

PN adsorption on the reference and catalysts supports was performed using pressed disks of the pure support powders, previously outgassed in IR cell, which was connected to a conventional gas manipulation–evacuation apparatus. These measurements were performed at room temperature, with 100 scans and 4 cm^{-1} resolution on a Magna 760-IR spectrophotometer by Nicolet.

2.3. Catalyst preparation

The catalyst was prepared by pore volume impregnation using an aqueous solution of AHM $(NH_4)_6Mo_7O_{24}{\cdot}4H_2O$ (Merck, AR) with the necessary concentration to reach

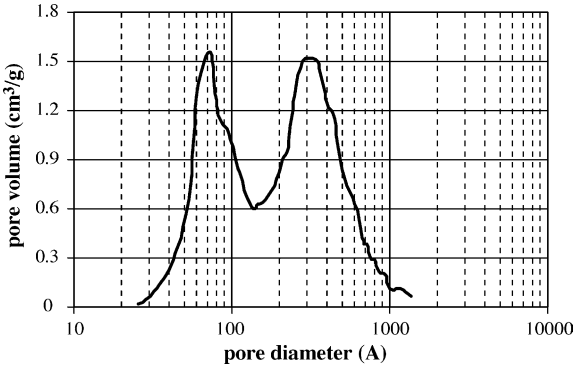

Fig. 2. Pore volume distribution for the mixed oxide Al_2O_3–TiO_2 used as support.

Table 1
Experiments for the HDM of Ni-TPP

Test	Ni (ppm)	Catalyst weight (mg)
Ni-1	20	40
Ni-2	20	35
Ni-3	10	20

7 wt.% molybdenum. The catalysts precursor was dried at 100 °C for 24 h and calcined at 450 °C by 4 h.

2.4. Ni-TPP in nujol solution preparation

Mineral oil (nujol) of relatively high viscosity and boiling point, free of sulfur and nitrogen was used as solvent. The solvent and the required amount of Ni-TPP (Fisher R.A.) porphyirin were warmed up under Argon (Praxair UAP) flow from room temperature to 80 °C. The temperature was held at 80 °C for 1 h to eliminate dissolved oxygen in the solvent. The solution was then warmed up to 300 °C and maintained at this temperature during 4 h. Then the solution was cooled to room temperature and filtered. The resultant solution contained 20 ppm (weight) of Ni.

2.5. Catalytic evaluation

Before use, the catalyst was ground and meshed to 0.074–0.088 mm size particles to avoid internal mass and energy transport limitations [5]. Prior to its use in the reactions, the catalyst was sulfided ex situ with a H_2S (15%, v/v)/H_2 gaseous mixture at 400 °C for 4 h. The HDM kinetic experiments were carried out in a 300 mL Parr batch reactor. For each experiment, 100 mL of porphyrin solution was loaded into the reactor, filled with argon. Later, the reactor was purged and pressurized to 8.3 MPa with hydrogen. In these conditions, the reactor was heated to the reaction temperature (325 °C). Liquid samples were taken hourly and were analyzed on a Varian Cary 5 UV–vis spectrometer. The concentrations of the porphyrin and its hydrogenated intermediate compounds were computed applying the Lambert–Beer law. The molar absorptivity coefficient (ε) for Ni-TPP was determined from the calibration curve made with standard solutions of the pure compound. The absorption coefficients of the intermediate compounds were calculated using the absorbance versus time curves from data from literature [11]. A summary of the Ni-TPP HDM tests made in this work appears in Table 1.

Several proposed models were evaluated and the kinetic parameters were obtained from the concentration versus time experimental curves. A mathematical fit for each model was achieved using the Micromath Scientist® nonlinear regression software. The objective function, defined as the sum of the squares of deviations between experimental and calculated concentrations, was minimized using a combination of Simplex and Levenberg–Marquardt methods. Fourth order Runge–Kutta method was employed to solve the DOE set generated by each kinetic model.

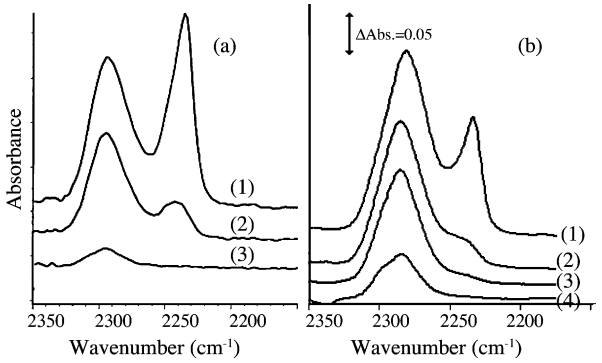

Fig. 3. FT-IR spectra of adsorbed pivalonitrile. (a) Reference alumina; (b) Al_2O_3–TiO_2 support. (1) PN adsorbed at room temperature; (2) outgassed at room temperature; (3) outgassed at 100 °C; (4) outgassed at 200 °C.

3. Results and discussion

The acidity of Al_2O_3 and Al_2O_3–TiO_2 supports was evaluated by the adsorption of pivalonitrile (PN) as probe molecule followed by FT-IR analysis. The resulting FT-IR spectra for both support samples are shown in Fig. 3.

According to literature, upon adsorption of PN on an alumina based support two bands appear at 2235 and 2295 cm^{-1}. The first one could be ascribed to weakly adsorbed hydrogen bond species [12]. Outgassing at high temperatures leaves a band present with a maximum at 2295 cm^{-1} and also reveals a higher frequency component near 2305 cm^{-1}. These bands can be assigned to pivalonitrile species bonded to two types of Lewis acid sites of alumina [13].

The spectrum of the species arising from pivalonitrile adsorption on the alumina reference sample shows two bands, centered at 2235 and 2295 cm^{-1}, respectively. The intensity of the lower frequency band diminishes drastically upon outgassing at room temperature and disappears almost completely upon evacuation at 100 °C, confirming the weak bonding of the adsorbed species. The higher frequency band decreases more slowly under outgassing and at 100 °C a small amount of PN still remains adsorbed.

For Al_2O_3–TiO_2 the former adsorption bands are identified. However, the spectrum at 100 °C shows interesting features, at this temperature the band located at 2235 cm^{-1} remains as a small shoulder and the band associated to Lewis acid sites shows grater intensity than the same band in the alumina reference; in fact, even at 200 °C this band remains clearly present. Thus, it can be concluded that Al_2O_3–TiO_2 has stronger acid sites centers of both types, Brønsted and Lewis than alumina.

A typical UV–vis absorption spectrum, obtained from a sample collected during the HDM reaction of Ni-TPP (Ni-1 test), is shown in Fig. 4. Two intense absorption bands are

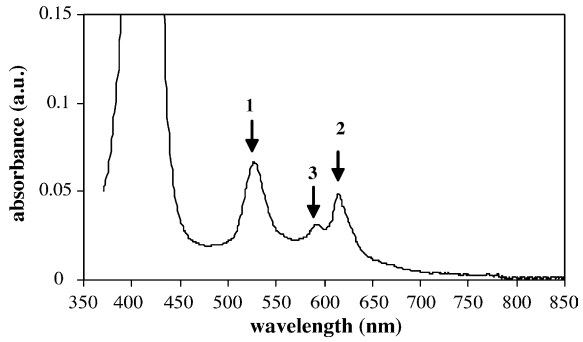

Fig. 4. UV–vis absorption spectrum for a single sample taken during the HDM reaction of Ni-TPP (Ni-1) test. The absorption bands of 1—Ni-TPP, 2—Ni-TPC, 3—Ni-TPiB are displayed.

observed, the first one located at 527.1 nm (1) and the second one at 615 nm (2). A shoulder is also observed at 592.9 nm (3). On the basis of the literature data [6,14], the absorption bands at 527.1 and 615 nm were assigned to Ni-TPP and to its dehydrogenated compound, nickel 5,10,15,20-tetraphenylchlorin (Ni-TPC), respectively. The shoulder at 592.9 nm is an absorption band characteristic of nickel 5,10,15,20-tetraphenylisobacteriochlorin (Ni-TPiB) [6].

The concentration versus reaction time plot for the Ni-1 test is displayed in Fig. 5. A continuous decrease is observed in the Ni-TPP concentration with time; whereas, Ni-TPC and Ni-TPiB concentrations increase and, after reaching a maximum value, diminish slowly. The same trend was also observed in the Ni-2 and Ni-3 tests. This behavior suggests that Ni-TPC and Ni-TPiB are intermediate compounds in the consecutive overall Ni-TPP HDM reaction. This observation is in agreement with the chemistry of metalloporphyrins, which under conditions of chemical reduction can be hydrogenated several times successively until the macromolecule of porphyrin is broken, losing its porphyrinic character [15].

On the basis of the observed behavior of Ni-TPP HDM, in which only two hydrogenated reaction intermediates were

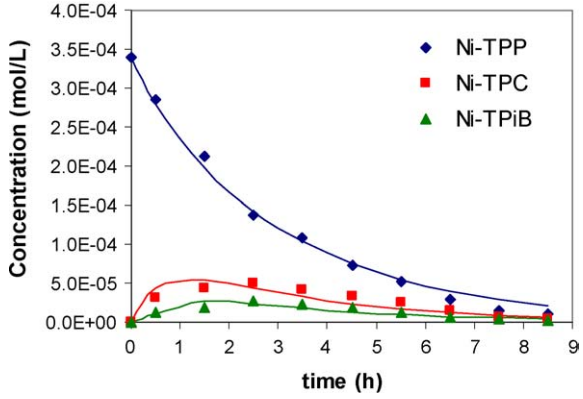

Fig. 5. Variation of concentration against time for Ni-TPP (Ni-1) HDM reaction. (Symbols) experimental values. (—) Calculated values from model 1.

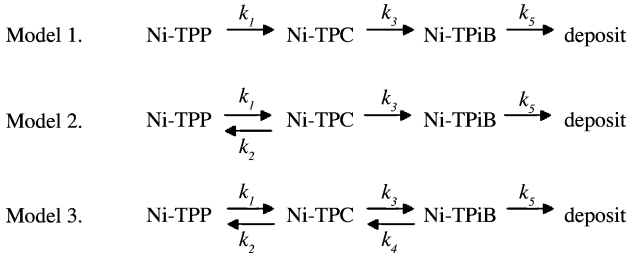

Fig. 6. Proposed kinetic models for Ni-TPP HDM reaction.

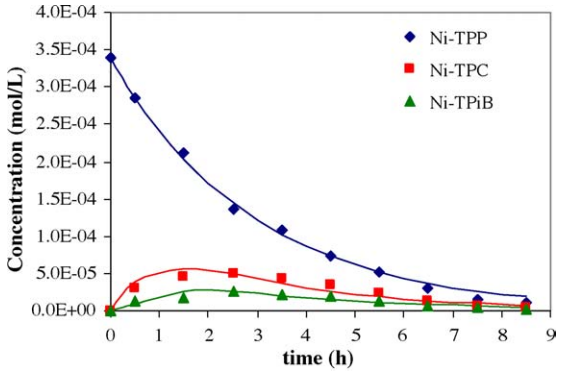

Fig. 7. Concentration vs. reaction time for Ni-TPP (Ni-1) HDM. (Symbols) experimental values. (—) Calculated values from model 2.

detected (Ni-TPC and Ni-TPiB), three consecutive reaction schemes can be proposed to fit the experimental data. The proposed reaction models are detailed in Fig. 6. All the reaction steps in the models were assumed to be first order with respect to porphyrinic species concentrations (Ni-TPP, Ni-TPC and Ni-TPiB). It was also assumed that the hydrogen concentration in the nujol solvent remains constant during the HDM reaction.

The mathematical fitting of the data using models 1 and 2, for the Ni-1 test, appear in Figs. 5 and 7, respectively. A summary of the estimated kinetics parameters is presented in Table 2. The correlation coefficients for each fitted curve are given in Table 3. Although model 1 fits the experimental Ni-TPP and Ni-TPiB concentrations relatively well, it has some deviation respect to the Ni-TPC concentrations, especially

Table 2
Rate coefficients for Ni-TPP HDM, from proposed kinetic models

Rate coefficients	Model 1	Model 2	Model 3
k_1	0.4298	0.3433	0.3482
k_3	1.3221	1.2506	3.6660
k_5	2.6352	2.5804	2.5070

Table 3
Correlation coefficients for three models

Adjusted curve	R^2		
	Model 1	Model 2	Model 3
Ni-TPP	0.9796	0.9778	0.9783
Ni-TPC	0.9096	0.9216	0.9522
Ni-TPiB	0.9243	0.9368	0.9365

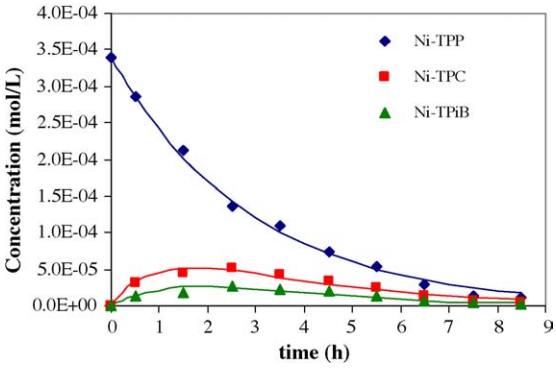

Fig. 8. Concentration vs. reaction time for Ni-TPP (Ni-1) HDM. (Symbols) experimental values. (—) Calculated values from model 3.

for long reaction times. This suggests that the first hydrogenation step is reversible. Taking into account this possibility, model 2 includes a reversible first hydrogenation step. This adjustment to the model slightly improves the fit of the experimental data, suggesting that the first hydrogenation step is reversible.

Model 3, which includes two reversible hydrogenation steps and an irreversible hydrogenolysis step, fits the experimental concentrations very well for all the porphyrinic species (Ni-TPP, Ni-TPP and Ni-TPiB), indicating that this consecutive mechanism is suitable to model the HDM kinetics of Ni-TPP. The fit of this model to the experimental data is presented in Fig. 8 and the correlation coefficients are given in Table 3. The rate expressions for this mechanism are given in Fig. 9.

The previous results can be summarized as follows: under our experimental conditions using a Mo/Al_2O_3-TiO_2 catalyst, Ni-TPP reacts through a sequential mechanism with two reversible hydrogenation steps. In the first step, Ni-TPP is hydrogenated to form Ni-TPC, which is subsequently hydrogenated to form the tetrahydrogenated intermediate, Ni-TPiB. Finally, in agreement with previously reported data, it is assumed that Ni-TPiB reacts through a series of fast reactions, resulting in loss of the aromatic character for the porphyrin macromolecule that facilitates the demetallation and fragmentation of the porphyrinic ring. The previous mechanism is in good agreement with the mechanisms of Ni-TPP HDM proposed by other researchers [6,9,11,16,17] for alumina-supported catalysts.

Investigations on the HDM of TPP type porphyrins with Mo or CoMo catalysts supported on γ-Al_2O_3, reported the hydrogenolysis of the Ni–N bonds as the rate-limiting step

$$\frac{dC_{Ni-TPP}}{dt} = k_2 C_{Ni-TPC} - k_1 C_{Ni-TPP}$$

$$\frac{dC_{Ni-TPC}}{dt} = k_1 C_{Ni-TPP} + k_4 C_{Ni-TPiB} - (k_2 + k_3) C_{Ni-TPC}$$

$$\frac{dC_{Ni-TPiB}}{dt} = k_3 C_{Ni-TPC} - (k_4 + k_5) C_{Ni-TPiB}$$

Fig. 9. Kinetic rate expression used in model 3.

[6,9,11,16,17]. However, with the catalyst used here and under our operating conditions, the controlling HDM step was the first hydrogenation of Ni-TPP (k_1) instead of hydrogenolysis of the Ni–N bond in Ni-TPiB (k_5) (see Table 2). This different behavior with respect to alumina-supported catalysts can be explained on the basis of the surface acidity of the catalysts used here.

Yang [18,19], in a kinetic study on quinoleine HDN, postulated the existence of two types of active sites on a sulfided $NiMo/Al_2O_3$ catalyst: (1) Sulfur vacancies, associated with Mo (acid Lewis sites), and (2) Brønsted acid sites, resulting from the dissociative adsorption of H_2S on the sulfur vacancies. It was claimed that the sulfur vacancies are responsible for the hydrogenation and hydrogenolysis reactions, whereas the Brønsted acid sites are responsible for the hydrogenolysis reactions.

The Al_2O_3–TiO_2 support used in the catalyst displays stronger acid sites than alumina. Therefore, one expects stronger acid sites, in a sulfided Mo/Al_2O_3-TiO_2 than in a similar Mo/γ-Al_2O_3 catalyst. The fact that the best fitting model indicates that the rate determining step is the hydrogenation rather than the hydrogenolysis, reported for alumina supported catalysts, indicates that the greater acidity of the sulfided Mo/Al_2O_3-TiO_2 is responsible for this change in rate determining step, in agreement with the proposals of Yang [18,19].

4. Conclusions

For a sulfided Mo/Al_2O_3-TiO_2 catalyst and under our experimental conditions:

1. Ni-TPP proceeds via a consecutive mechanism with three reaction steps. In the first step, Ni-TPP is reversibly hydrogenated to form Ni-TPC. This compound is also reversibly hydrogenated to form the tetrahydrogenated Ni-TPiB. Finally, Ni-TPiB reacts through a series of fast reactions that lead to the demetallation and fragmentation of the ring.
2. With the support used here, the rate-controlling step for the overall Ni-TPP demetallation scheme was the first hydrogenation (k_1) instead of the hydrogenolysis step (k_5). This can be explained based on the higher acidity of the Mo/Al_2O_3-TiO_2 catalyst respect to the Mo/Al_2O_3 catalyst.

Acknowledgements

The authors wish to thank V. Martínez for the preparation and IR pivalonitrile of the Al_2O_3–TiO_2 support. Also authors are grateful to the Mexican Institute of Petroleum by financial support through project FIES 98-113-II. J. García thanks to CONACyT for the scholarship to attend his MSc studies.

References

[1] P.W. Tamm, H.F. Harnsberger, A.G. Bridge, Ind. Eng. Chem. Process Des. Dev. 20 (1981) 262.
[2] S.M. Oleck, H.S. Sherry, Ind. Eng. Chem. Process Des. Dev. 16 (1977) 525.
[3] C.D. Chang, A.J. Silvestri, Ind. Eng. Chem. Process Des. Dev. 15 (1976) 161.
[4] C.W. Hung, J. Wei, Ind. Eng. Chem. Process Des. Dev. 19 (1980) 250.
[5] R. Agrawal, J. Wei, Ind. Eng. Chem. Process Des. Dev. 23 (1984) 505.
[6] R.A. Ware, J. Wei, J. Catal. 93 (1985) 100.
[7] B.J. Smith, J. Wei, J. Catal. 132 (1991) 1.
[8] H.J. Chen, F.E. Massoth, Ind. Eng. Chem. Res. 27 (1988) 1629.
[9] R.L.C. Bonné, P. Steenderen, A.D. Van Langeveld, J.A. Moulijn, Ind. Eng. Chem. Res. 34 (1995) 3801.
[10] J. Ramírez, G. Macias, L. Cedeño, A. Gutiérrez-Alejandre, R. Cuevas, P. Castillo, Catal. Today 98 (1–2) (2004) 19.
[11] R.L.C. Bonné, P. van Steenderen, J.A. Moulijn, Appl. Catal. A 206 (2001) 171.
[12] A. Gutiérrez-Alejandre, M. González-Cruz, M. Trombetta, G. Busca, J. Ramírez, Micropor. Mesopor. Mater. 23 (1998) 265.
[13] H. Knözinger, H. Krietenbrink, J. Chem. Soc., Faraday Trans. I 71 (1975) 2421.
[14] G.D. Dorough, J.R. Miler, F. Huennekens, J. Am. Chem. Soc. 74 (1952) 3974.
[15] R.H. Scheer, in: D. Dolphin (Ed.), The Porphyrins, vol. II, Academic Press, New York, 1978 (Chapter 1).
[16] R.L.C. Bonné, P. van Steenderen, J.A. Moulijn, Bull. Soc. Chim. Belg. 100 (11–12) (1991) 877.
[17] R.L.C. Bonné, P. van Steenderen, A.E. van Diepen, J.A. Moulijn, Appl. Catal. A 108 (1994) 171.
[18] S.H. Yang, C.N. Satterfield, J. Catal. 81 (1983) 168.
[19] S.H. Yang, C.N. Satterfield, Ind. Eng. Chem. Process Des. Dev. 23 (1984) 20.